BOLETIN DE LA SOCIEDAD ESPAÑOLA DE
Cerámica y Vidrio
www.elsevier.es/bsecv

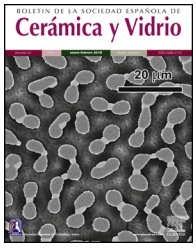

Study of the interaction between low density polyethylene and TiO_2 in different environments. Influence of the presence and absence of radiation, and of the atmosphere (O_2, N_2 or Ar)

Ana Castellanos-Aliaga[a,b,*], *Laura San-Miguel*[a], *Marina Villegas*[a], *Ángel Caballero*[c], *Marco Peiteado*[a], *David González Calatayud*[a,b]

[a] *Department of Electroceramics, Instituto de Cerámica y Vidrio (CSIC), Kelsen 5, 28049 Madrid, Spain*
[b] *Department of Inorganic Chemistry, Universidad Autónoma de Madrid, Francisco Tomás y Valiente 7, 28049 Madrid, Spain*
[c] *Department of Ceramics, Instituto de Cerámica y Vidrio (CSIC), Kelsen 5, 28049 Madrid, Spain*

ARTICLE INFO

Article history:
Received 1 July 2024
Accepted 16 September 2024
Available online 4 October 2024

Keywords:
TiO_2
Catalysis
Photocatalysis
Degradation of plastics
LDPE

ABSTRACT

In the process of photocatalytic degradation of plastics, the surface interaction between the plastic material and the photocatalyst results crucial. The present work focuses on using a specific TiO_2 photocatalytic semiconductor whose hierarchical structure favours the interaction with low density polyethylene (LDPE), a key component in plastics. An exhaustive study of the nature of this interaction is conducted, analysing the influence of the atmosphere and radiation. The results obtained indicate that the observed interaction can be modulated by controlling the atmosphere, evolving into a degradation process whose mechanism also depends on the absence or the presence of light. This point is particularly relevant as it highlights the dual nature of TiO_2 as both photocatalyst and catalyst.

Estudio de la interacción entre el polietileno de baja densidad y el TiO_2 en distintos ambientes. Influencia de la presencia y ausencia de radiación, así como de la atmósfera (O_2, N_2 y Ar)

Palabras clave:
TiO_2
Catálisis
Fotocatálisis
Degradación de plásticos
LDPE

RESUMEN

En el proceso de degradación fotocatalítica de plásticos, la interacción superficial entre el material plástico y el fotocatalizador resulta crucial. El presente trabajo se centra en la utilización de un semiconductor fotocatalítico específico de TiO_2 cuya estructura jerárquica favorece la interacción con el polietileno de baja densidad (LDPE), componente clave de los plásticos. La naturaleza específica de la interacción entre ambos materiales se estudia de manera exhaustiva y en función tanto de la atmósfera como de la radiación aplicadas.

* *Corresponding author.*
E-mail address: ana.castellanos@icv.csic.es (A. Castellanos-Aliaga).
https://doi.org/10.1016/j.bsecv.2024.09.005

Los resultados obtenidos indican que la interacción observada se puede modular mediante el control de la atmósfera, evolucionando hacia un proceso de degradación cuyo mecanismo también depende de la ausencia o presencia de luz. Este punto es especialmente relevante ya que pone de manifiesto la naturaleza dual del TiO_2 como fotocatalizador y como catalizador.

Introduction

Low production cost combined with high durability, versatility, malleability, lightness and many other properties, have made plastics a material of great economic, technological and industrial interest, being one of the most widely used materials worldwide. This widespread use also generates a large amount of waste which is tricky to manage, leading to a worrisome accumulation, also known as plastic pollution. In fact, only a 21% of the 6300 Mt. of plastic waste generated since 1950 has been removed [1]. A standard plastic material is mainly based on an organic polymer macromolecule formed by monomers that are produced synthetically or by natural product conversion. However, it takes a long time to naturally degrade plastics, and the process ultimately ends in the release of different additives, as well as the fragmentation of plastics into smaller sizes that can be ingested by living organisms. Among the most common additives are antioxidants such as hindered amine light stabilizers (HALS), or bisphenol A (BPA) and phthalates to develop several properties. Some of these are considered endocrine disrupting chemicals and can leach from plastic items [1]. In addition, plastics can adsorb toxic metals, which amplifies their toxicity in food chains, altering the microbial community structure and obscuring ecosystem functioning [2,3]. Among all the different types of plastics used, polyethylene (PE) is one of the most popular. Specifically, low density polyethylene (LDPE) accounts for 20% of plastic waste [2,4]. This polymer is based on the repetition of ethylene creating ramifications and it is also reported to have HALS stabilizers in its formulation. These stabilizers are derivatives of 2,2,6,6-tetramethylpiperidine and related compounds and their function is to prevent the polymer from photo-oxidation [5].

Several approaches have been studied to address the challenge of plastic waste. In this context, advanced oxidation processes (AOPs) are among the most promising alternatives. They are based on the generation of reactive oxygen species (ROS) like hydroxyl ($HO\bullet$) and/or peroxide radicals ($O_2\bullet^-$) to react with organic pollutants *via* radical reactions [6]. One of the most effective AOP strategies is photocatalysis, based on the use of a light source to irradiate a semiconductor which then generates electron–hole pairs. These species are reported to react respectively with oxygen and water (and/or hydroxyl groups) adsorbed on the surface. This generates radicals that can initiate the photodegradation of organic compounds [7,8]. However, several limitations of this process are addressed. First, the efficiency of the process is reduced for film-shape and/or large-size plastics. A plastic film configuration hinders the absorption of photons by the semiconductor, thereby reducing its capacity to produce ROS. In terms of polymer size, the larger the molecule, the more its adsorption on the surface of the semiconductor is impeded. Being a surface effect, it also depends on semiconductor characteristics such as specific surface area, particle size, porosity, crystallinity and band gap [9,10], which makes the selection of the semiconductor critical for an effective response. In this work, we aim to study the possibilities of plastic degradation using titanium dioxide (TiO_2), a ceramic semiconductor frequently used in photocatalytic degradation processes and water decontamination treatments [11,12]. In fact, its strong oxidising power, good chemical stability and low cost are *a priori* very suitable for effective polyethylene degradation, as it has been recently reported [13–15]. Most of these works focus on the degradation mechanisms of TiO_2 in solution, but few studies have dealt with its behaviour in the solid state, even though almost 80% of plastic waste is accumulated as soil [1]. In what follows, this solid-state surface-based reactivity will be analysed, further evaluating the role of the atmosphere and radiation in the expected TiO_2–LDPE interaction.

Experimental procedure

The LDPE plastic material studied in this work is a Labbox AstiK flat zip bag, 8 cm wide × 14 cm high, with an average thickness of 50 μm. As for the photocatalyst, a highly reactive TiO_2 ceramic powder obtained by a simple synthesis process previously developed and patented by the research team was used [16–18]. In essence, a solution of titanium (IV) tetrabutoxide and trifluoroacetic acid in 1 L of absolute ethanol is stirred for 6.5 h at room temperature and then evaporated to dryness under atmospheric conditions. After subsequent washing, the white precipitate obtained consists of nanostructured mesoporous microspheres, with a high specific surface area that can facilitate the interaction with the plastic surface. The experimental setup for the interaction studies can be described as follows: for the tests under darkness, a spatula tip (~60 mg) of the synthesised TiO_2 powder is placed inside the LDPE bag. The system is stored in total darkness for 27 days. Three different atmospheres were tested in darkness experiments, namely air ($O_2/N_2/H_2O$), pure N_2 and pure Ar. In the case of inert atmospheres, the TiO_2-containing bags were put under vacuum for several minutes and then filled with the required gas. The same procedure was repeated for the experiments under light, but this time the bag-TiO_2 couples were exposed to UVA–visible radiation during 27 days under air atmosphere. An empty bag was also irradiated as a reference.

For these light tests, a System Photolab LED365-14/450-12c (APRIA Systems S.L.) was used. It consists of a 10 cm × 10 cm cell with an irradiated area of 100 cm^2. The cell is placed 40 cm away from the irradiation source, which is provided with visible (λ = 400–700 nm) and UV-A (λ = 365–370 nm) LEDs. The LEDs setting chosen was 100% UV-A and 25% visible with a total of 1800 lumens. In both the darkness and light tests, the samples are weighed before and after the test, and the difference is normalised with respect to the amount of ceramic powder introduced in the bag. Once the 27 days are completed, the ceramic powder is carefully removed from the bag and the latter is cut into 1 cm × 1 cm slides. A differentiation is made between the inner side of the plastic in contact with the ceramic powder and the outer side. Finally, the plastic pieces are softly cleaned with distilled water and dried with paper.

An in-depth characterisation of each sample is carried out before and after the experiments. The functional groups of LDPE and TiO_2 were studied by FTIR-ATR using a PerkinElmer precisely Spectrum 100 FT-IR Spectrometer with a Pike Technologies GladiATR™ module. Samples are pressed with a diamond crystal to obtain a scan from 4000 to 400 cm^{-1}. The internal electronic band structure of TiO_2 was analysed by emission of photoluminescence using a Spectrofluorometer FS5 from Edinburgh Instruments with a Xe+UV lamp of 150 W (λ = 200–1000 nm). Specifically, the excitation wavelength is fixed at 230 nm with an excitation bandwidth of 5 nm, whereas the emission scan goes from 340 to 475 nm and the emission bandwidth is 1 nm. A single repeat scan is obtained, with a step of 0.10 nm and a dwell time of 1.50 s. A short pass filter of 450 nm is placed before the sample. The spectrum obtained is deconvoluted and the emission bands are normalised with respect to the band gap band. Morphology studies were conducted using a field-emission scanning electron microscope (FESEM, Hitachi S-4700). Due to the insulating polymeric nature of LDPE, samples were prepared applying an Au sputtered coating. TiO_2 particles were also analysed by transmission electron microscopy (TEM, JEOL 2100F). The crystallinity of LDPE and TiO_2 was determined on an XRD Bruker D8-Advance powder diffractometer with monochromatised Cu Kα1 radiation (1.54060 Å) and a Lynx Eye detector. FTIR measurements were conducted on a JASCO FT/IR-4X spectrometer. Since plastic films usually have parallel surfaces, when an IR beam interacts with them, constructive and destructive interferences can occur and a "fringing effect" is observed in the FTIR spectrum [19]. In our case, the "fringing effect" comprised between 1352 and 1019 cm^{-1} frequencies was selected. The thickness of the plastic (b) was obtained using the following equation, where n is the LDPE refractive index, N is the number of fringes in the given spectral region and υ is the frequency.

$$b = \frac{1}{2n} \cdot \frac{N}{(\upsilon_1 - \upsilon_2)} \quad (1)$$

The percentage of carbon in the LDPE samples before and after the experiments was scrutinised with an Elemental Analyzer LECO CHNS-932, whereas the band gap of the semiconductor TiO_2 was calculated using an Analytik-Jena Specord 200 Plus spectrophotometer equipped with deuterium (UV, 190–318 nm) and tungsten (UV–visible, 318–1100 nm) lamps. For band gap calculation a slow scan of 190–900 nm was carried out and the TiO_2 samples were placed inside an integrating sphere for diffuse reflectance of 120 mm. A deconvolution of the λ *vs* absorbance obtained plot was done to remove any contribution of the colour of the powder. The absorbance of the band gap signal is converted into reflectance and then the Kubelka–Munk algorithm is applied to obtain the absorption coefficient (α). From this value, the Tauc plot for a permitted indirect band gap ($(\alpha hn)^{1/2}$ *vs* hn) is plotted and the band gap is then calculated by extrapolating the linear region to zero. Finally, the specific surface area of the semiconductor was determined by the Brunauer–Emmett–Telle (BET) method in an ASAP 2020-Micromeritics (Norcross, GA, USA) at 77 K. Nitrogen adsorption/desorption isotherms were carried out on an ASAP 2020-Micromeritics (Norcross, GA, USA) at 77 K. Samples were degassed at 30 °C during 48 h before analysis.

Results and discussion

Synthesis and characterisation of the TiO_2 ceramic material

Fig. 1 shows the main characteristics of the as-synthesised TiO_2 powder (Fig. 1a–c) together with the experimental setup of the bag-TiO_2 couple samples (Fig. 1d and e). As mentioned, the interaction between the plastic material and the surface of the photocatalyst is highly dependent on the specific characteristics of the latter, including particle size, specific surface area, porosity, crystallinity, chemical composition and, in the case of a semiconductor such as TiO_2, also the band gap. Regarding the size, the experimental procedure described in "Experimental procedure" section results into a product that maintains a nanostructured micron-sized spherical geometry (Fig. 1a and b). Specifically, the size of the nanoparticles is in the range between 2 and 10 nm but they are hierarchically assembled to form a sphere with a diameter of 1–3 μm. The small size of the nanoparticles, close to the quantum dots (QDs) range, is meant to enhance the photocatalytic activity of TiO_2. But simultaneously, as they are organised into a micrometric sphere, their sticky typical agglomeration that causes losses in photocatalytic activity by reduction of the accessible active sites is avoided. In addition, the micrometric size facilitates the handling of the material, reduces its toxicity [20] and favours the interaction between the plastic and the photocatalyst, which is normally limited by the large size difference between both materials [1]. In terms of specific surface area, the larger its value, the better interaction, and thus a more effective degradation would be expected [21]. A specific surface area as high as 180.19 m^2/g with an average pore size of 3.2 nm (Fig. S1) is reached with this synthesis routine; nevertheless, it is necessary to point out that due to the very nature of the hierarchical structure, the name "pores" does not refer to channels but rather the spaces generated between the nanoparticles upon assembling.

As it can be observed by TEM and X-ray powder diffraction, the synthesis procedure also stabilises the most unstable polymorph of TiO_2, brookite, allowing its coexistence with the most reactive anatase phase (Fig. 1b and c). The coexistence of both polymorphs can actually lead to interfacial homojunctions in which electrons can transfer from brookite to

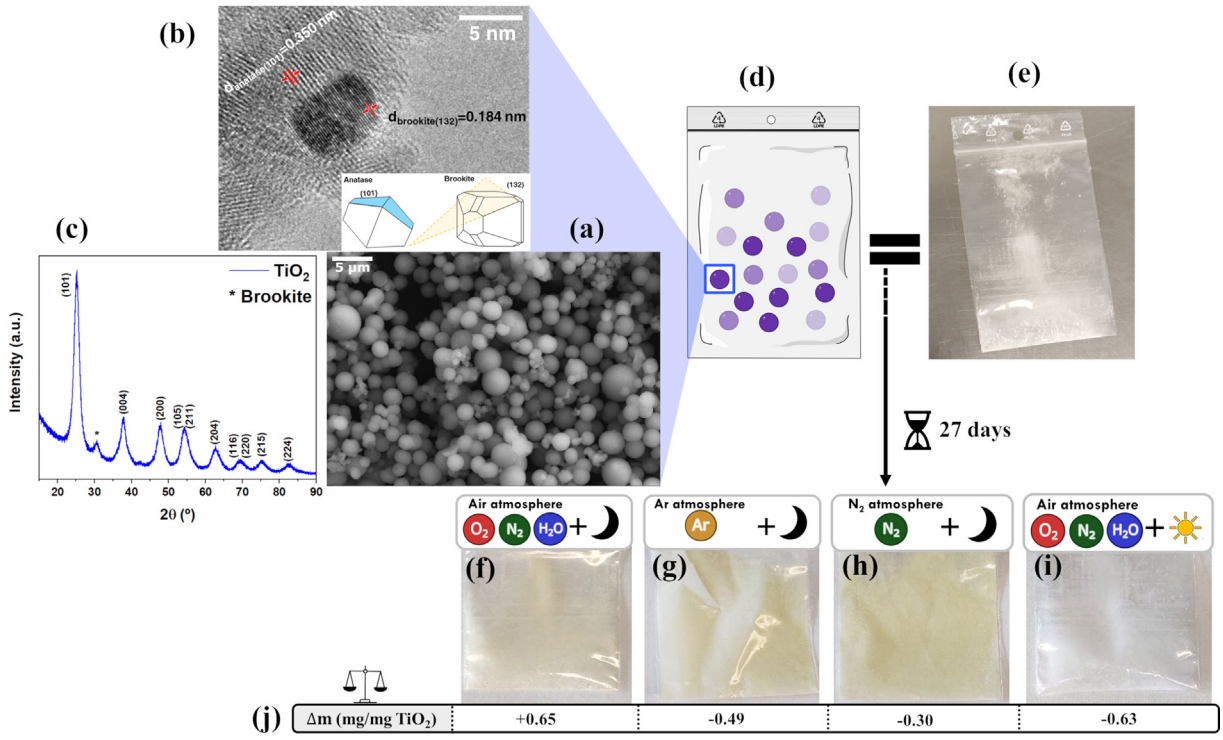

Fig. 1 – (a) Morphology of the TiO_2 microspheres synthesised as observed by FE-SEM; (b) TEM micrograph of the nanoparticles that conform the TiO_2 sphere. Interplanar distance of anatase and brookite are observed; (c) X-ray diffractogram of the synthesised TiO_2 powder before contacting with LDPE. All diffraction maxima indexed correspond to anatase phase (#00-021-1272). The diffraction maximum of brookite phase (#00-029-1360) is marked with the symbol (*); (d) graphical representation and (e) digital photograph of LDPE–TiO_2 initial experimental system. Digital photograph of LDPE–TiO_2 final experimental system after 27 days in: (f) air and darkness, (g) Ar and darkness, (h) N_2 and darkness, (i) air and UVA radiation environments; (j) difference in weight between the final and initial system normalised with respect to the amount of TiO_2 initially added.

anatase, thereby decreasing the electron–hole recombination rate and enhancing the photocatalytic efficiency [22]. Moreover, according to optical measurements, the as-obtained TiO_2 particles displayed a reduced band gap of 3.04 eV (408 nm) (Fig. S2), which is also beneficial to increase the activity beyond the UV range [21]. Finally, FTIR-ATR measurements also indicate a high photoactivity situation in the synthesised TiO_2 powder. The black spectrum in Fig. 2c reveals the existence of asymmetric and symmetric C=O stretching vibrations resulting from the incorporation of TFAA (CF_3COOH) to the TiO_2 particles during the synthesis. Their specific positions at 1633 and 1440 cm^{-1}, respectively, further indicate that the TFFAA species are mainly bound to the Ti atoms in a bidentate (bridging or chelating) mode [7]. This is known to contribute to stabilise the {0 0 1} facets of anatase TiO_2, energetically unfavourable but certainly the most reactive, and thus photoactive, with 100% of the Ti atoms in five-fold coordination (Ti_{5C}) [7,9].

Study of the LDPE–TiO_2 interaction: air atmosphere + darkness

Usually, the pollutant and the photocatalyst are mixed in darkness to ensure a good contact before carrying out the irradiation [14]. Moreover, photolysis is sometimes considered the initial stage for the degradation of the polymer since UVA radiation has enough energy to break plastic bounds [23]. Therefore, to enable a good interaction between the two components and to avoid distortion of the results by photolysis, it is proposed to start by studying the LDPE–TiO_2 interaction under darkness in an air atmosphere. The first indication that an interaction has taken place is the yellow colouring of the semiconductor (initially white) after contacting with the plastic, while the bag remains transparent and colourless (Fig. 1e *vs* f). Yellowing of this semiconductor has been observed to occur when it is considered defective due to Ti^{3+}, titanium interstitial (Ti_i) and/or oxygen vacancies [24–26]. The presence of Ti^{3+} and Ti_i would decrease the band gap [24,26], but in our sample this value increases from the initial 3.04 eV to 3.25 eV after 27 days of testing (Fig. S2). Likewise, the oxygen vacancies cannot be said to have increased, since the relative intensity of the emission photoluminescence corresponding to this defect (449 nm) [27,28] does not increase with respect to the original powder; on the contrary, this relative intensity decreases (Fig. 2e), actually implying a decrease in oxygen vacancies when TiO_2 comes into contact with LDPE. Some other authors have observed this yellowing as a consequence of the formation of a peroxy titanate complex at the surface of the TiO_2, pointing towards a bidentate chelating of the peroxide (O_2^{2-}) to the Ti^{4+} [8,29]. This requires the formation of the anion O_2^{2-}

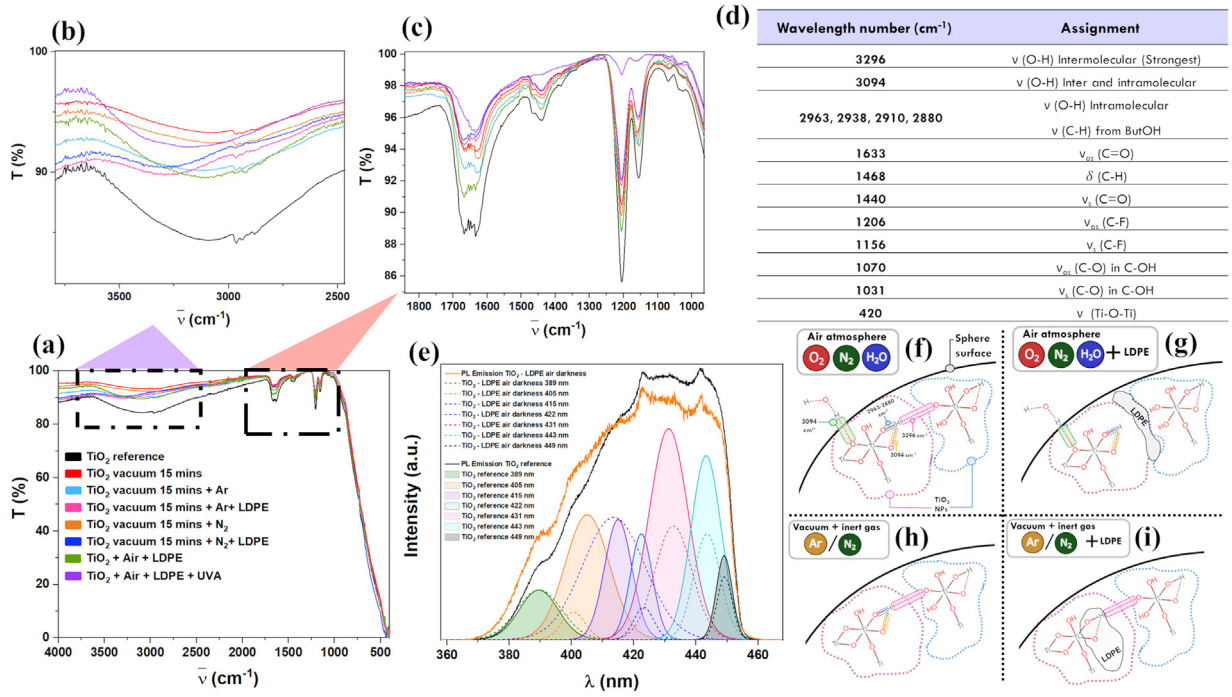

Wavelength number (cm^{-1})	Assignment
3296	ν (O-H) Intermolecular (Strongest)
3094	ν (O-H) Inter and intramolecular
2963, 2938, 2910, 2880	ν (O-H) Intramolecular ν (C-H) from ButOH
1633	ν_{as} (C=O)
1468	δ (C-H)
1440	ν_s (C=O)
1206	ν_{as} (C-F)
1156	ν_s (C-F)
1070	ν_{as} (C-O) in C-OH
1031	ν_s (C-O) in C-OH
420	ν (Ti-O-Ti)

Fig. 2 – (a) FTIR-ATR spectra of: TiO_2 synthesised before contacting LDPE in air atmosphere (black), under vacuum (red), under N_2 or Ar atmosphere (orange and light blue respectively) and TiO_2 synthesised after contacting LDPE with no radiation in air (green), N_2 (dark blue) and Ar (pink) environments. TiO_2 synthesised after contacting LDPE with UVA–vis radiation in air (purple). FTIR-ATR zoom spectra in (b) the 3500–2500 cm^{-1} ν(O—H) area and (c) 1750–1000 cm^{-1} TFAA coordination area. (d) Assignment of FTIR-ATR spectra bands. (e) Emission photoluminescence of TiO_2 powder before (black) and after (orange) contacting LDPE in air atmosphere under no radiation. The bands from the deconvolution of both signals (solid line filled bands and dashed lines respectively) are also shown. Scheme proposed of how the (f) initial ν(O—H) bands in air atmosphere are affected after applying an inert atmosphere (h) and after interacting with LDPE in those environments (g and i) respectively.

and its bonding to Ti^{4+}. A possible pathway could be related to the high electronegative fluorine atom of TFAA (CF_3COOH) coordinated on the surface. It has been already studied the capability of TFAA to produce radicals [30]. Therefore, we propose the abstraction of one electron of the double bond of the atmospheric oxygen by this functional group. The O_2• generated can react with another one to form the peroxy anion O_2^{2-} *via* radical reactions. As the nanoparticles of the spheres have the {0 0 1} facets with 100% Ti five-fold coordinated stabilised with TFAA but this acid is partially removed during the synthesis, the peroxy anion can easily coordinate to the defective titanium. This mechanism could weaken and/or displace the TFAA coordination, which is in accordance with the decrease of their band intensities observed by FTIR-ATR (Fig. 2c black *vs* green curves). As it has been previously described at the end of "Synthesis and characterisation of the TiO_2 ceramic material" section, Calatayud et al. [7] reported that the bidentate coordination of TFAA stabilised the {0 0 1} facets of anatase. Therefore, the loss of this coordination would be detrimental to the stabilisation of these facets. As a result, we propose that the unstable titanium present at the {0 0 1} facets will try to reduce its instability through a coordination with the ambient oxygen, which would partially fill the oxygen vacancies. Moreover, the formation of peroxy titanate could also partially fill the oxygen vacancies. In fact, as it has been previously mentioned, the relative intensity of the emission photoluminescence corresponding to this defect (449 nm) decreases when TiO_2 comes into contact with LDPE (Fig. 2e). This would imply an increase in the weight of the system, which is also observed (Fig. 1j).

Finally, different studies indicate that an increase of oxygen vacancies concentration induces a band tail near the conduction band that causes a reduction of the band gap [31,32]. Analogously, the decrease of oxygen vacancy would induce an increase of the band gap. This could explain why the original reduced band gap increases to 3.25 eV.

Looking back to the FTIR-ATR spectra (Fig. 2a), more remarkable is the decrease of the band at 3094 cm^{-1} corresponding to the υ(O—H) of the O—Ti—O—H and water adsorbed, and the fringes between 2963 and 2880 cm^{-1} related to the υ(C—H) ButOH from the synthesis adsorbed on pore and υ(O—H) intramolecular (Fig. 2b black *vs* green curves). As no temperature is applied in this process, these compounds can not evaporate. Therefore, the only way in which their concentration can be decreased is by desorption from the TiO_2 surface through the formation of radicals. As mentioned, TFAA may favour the formation of radicals, but its band intensity does not decrease so much as to be the architect behind the decrease of these radicals. Instead, titanium has to play a more predominant role. Its role as a photocatalyst and a

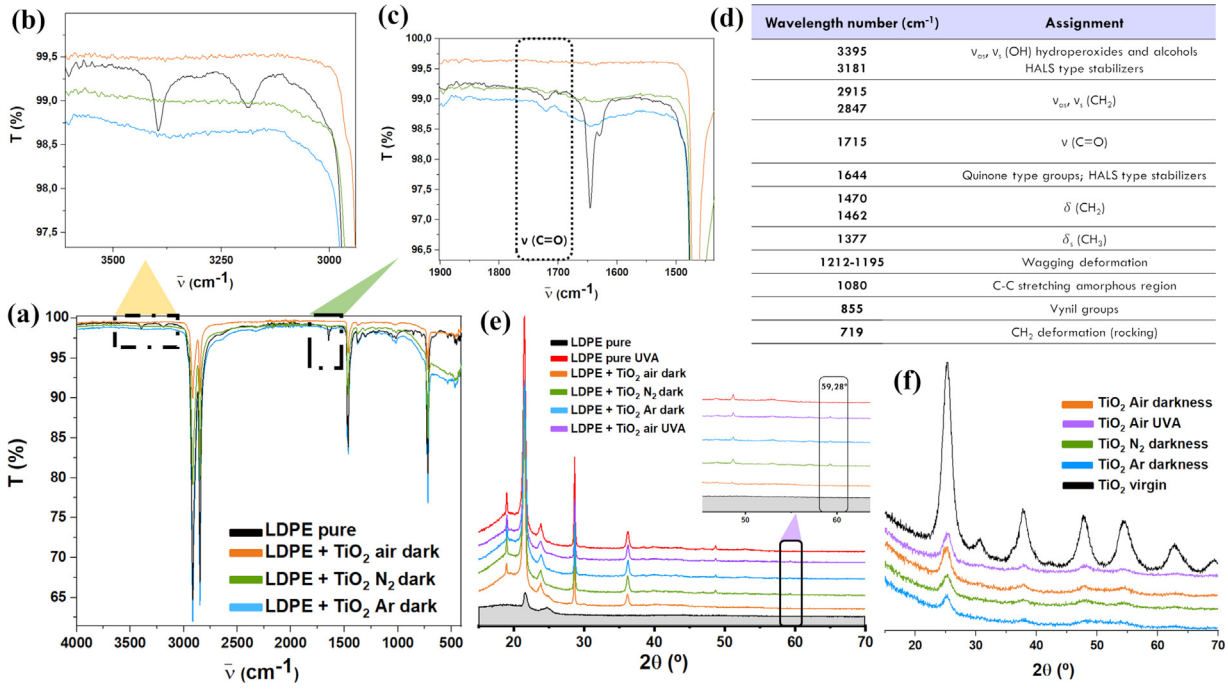

Wavelength number (cm^{-1})	Assignment
3395 3181	ν_{as}, ν_s (OH) hydroperoxides and alcohols HALS type stabilizers
2915 2847	ν_{as}, ν_s (CH_2)
1715	ν (C=O)
1644	Quinone type groups; HALS type stabilizers
1470 1462	δ (CH_2)
1377	δ_s (CH_3)
1212-1195	Wagging deformation
1080	C-C stretching amorphous region
855	Vynil groups
719	CH_2 deformation (rocking)

Fig. 3 – (a) FTIR-ATR spectra of LDPE before (black) and after 27 days of contact with TiO_2 in: air (orange), N_2 (green) and Ar (blue) atmospheres. FTIR-ATR zoom spectra in (b) the 3500–2500 cm^{-1} ν(O—H) and HALS area and (c) 1730–1600 cm^{-1} CO and HALS area. (d) Assignment of FTIR-ATR spectra bands. (e) X-ray diffractogram of: LDPE pure in darkness (black), LDPE pure under UVA light (red), LDPE after contacting TiO_2 under no radiation in: air (orange), N_2 (green) and Ar (blue) atmospheres, LDPE after contacting TiO_2 under UVA radiation in air atmosphere (purple). (f) X-ray diffractogram of TiO_2 powder before (black) and after contacting LDPE in: air (orange), N_2 (green) and Ar (blue) atmospheres under no radiation, and under UVA radiation in air atmosphere (purple).

support material for heterogeneous catalysis has been widely studied. However, its potential as a catalyst on its own is more unknown. As far to our knowledge, only a few authors have reported the ability of TiO_2 to produce radicals in the dark. Pirozzi et al. [33] reduce the oxygen of the air to a superoxo radical (O_2•$^-$) by an electron transfer from an acetylacetonate ligand to the semiconductor. In contrast, Fenoglio et al. [20] detected a favoured production of carbon-centred radicals in the dark by anatase nanoparticles through cleavage of C—H bonds. They also reported an enhancement of the reactivity of this polymorph under ambient illumination that generates oxygenated free radicals (HO_2•, O_2•$^-$, HO•). The latter should not be ruled out, because although the storage of the system was in complete darkness, the preparation was under ambient light. Since these radicals play a key role in the degradation of the polymer [14,15,33,34], their formation can be indirectly appreciated by looking at the changes in the FTIR-ATR spectra of the plastic (Fig. 3a). First, the LDPE virgin bag employed in this work presents in its formulation HALS type UV-stabilisers (bands at 3500–2900 cm^{-1} and 1644 cm^{-1}) (Fig. 3a–c black curves) [35], whose function is based on consuming the radicals formed during the plastic ageing process to prevent them from reacting with the polymer, thus protecting it. HALS form a nitroxide radical and then recover their initial structure *via* the Denisov cycle [5]. However, it seems that some of these HALS groups have been consumed since the plastic looks already aged, having carbonyl groups (1715 cm^{-1}) (Fig. 3c black curve) usually referred to as an indicator that the polymer degradation has begun [34,36–38]. When the titanium enters the equation, every band intensity of the functional groups of LDPE decreases and the HALS, carbonyl and vinyl bands disappear (Fig. 3a–c orange curves). Since no new bands of organic compounds are detected in the FTIR-ATR spectra of the powder (Fig. 2a green curve) and the plastic (Fig. 3a orange curve), it can be said that HALS stabilisers are depleted. Kamran et al. [6] established a possible mechanism for the degradation of a nitroxide radical in the presence of a HO• scavenger, MeOH. Since ButOH has been also identified as a HO• scavenger [39], we propose the same mechanism, being the nitroxide radical an already aged HALS stabiliser. As the stabilisers are depleted from the plastic, the polymer is no longer protected against oxidation. Therefore, we suggest a further oxidative attack of the polymer *via* HO• radicals generated by TiO_2. According to Llorente-García et al. [14], those radicals can initiate the degradation of the polymer by breaking the C—H bonds. The generated radicals can propagate by reacting with oxygen, chain imperfections and additives leading to different species like carbonyls [40]. These species along with the initial carbonyl ones could go to complex radical reactions leading to auto-oxidation. In an aerobic environment, this process tends to evolve towards chain scission rather than cross-linking [41]. Chain scission reduces the molecular weight of the polymer and increases the mobility of its amorphous phase [36]. This facilitates even more the easy

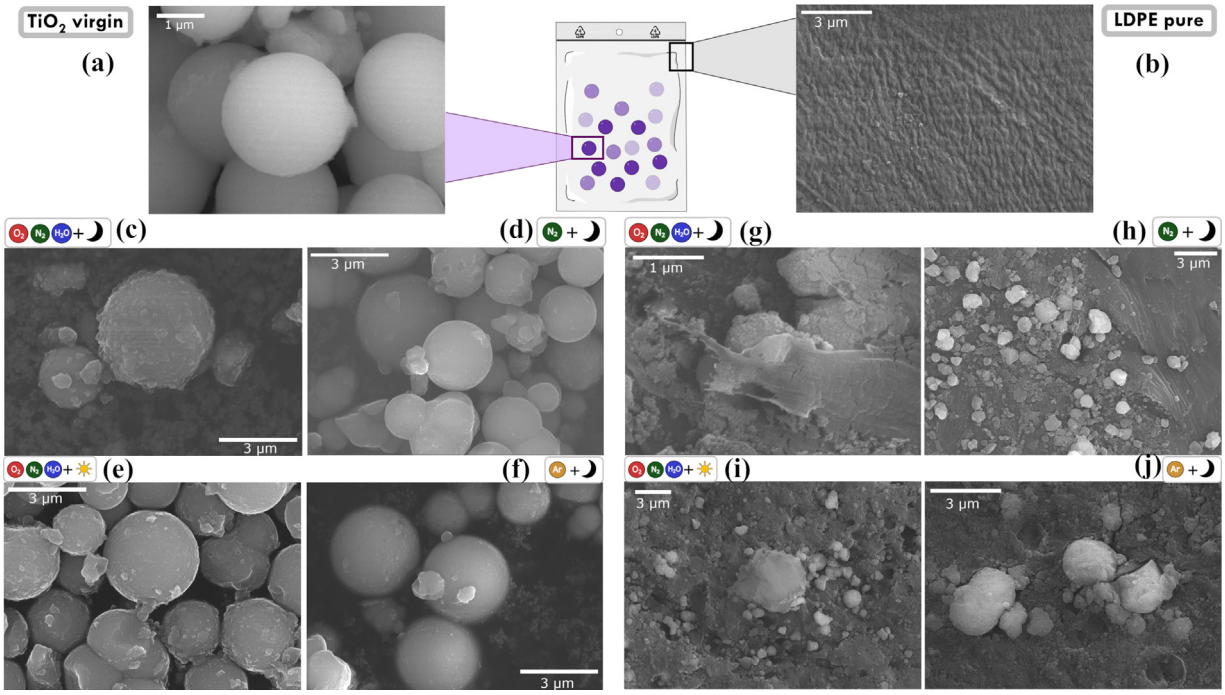

Fig. 4 – FE-SEM micrographs of the evolution of TiO_2 morphology before (a) and after contacting with LDPE under no radiation in air (c), N_2 (d) and Ar (f) atmospheres. (e) TiO_2 after contacting with LDPE under UVA light in air atmosphere. LDPE before (b) and after contacting TiO_2 under no radiation in air (g), N_2 (h) and Ar (j) atmospheres. (i) LDPE after contacting with TiO_2 under UVA light in air atmosphere.

movement of small radicals like HO• inside this phase [40]. Consequently, the propagation can continue deeper crystallising the polymer. In fact, far from being a negligible process, the crystallinity of the polymer increases considerably, with new diffraction maxima appearing (Fig. 3e) [42]. In contrast, the crystallinity of the semiconductor decreases after this interaction (Fig. 3f), which is closely related to the morphology obtained by FE-SEM (Fig. 4). The spheres that did not have such close contact with the plastic (Fig. 4c) have a similar morphology to the initial one (Fig. 4a) but with a surface completely covered by granules. This covering, along with the interaction between LDPE and TiO_2 previously described, could have caused an amorphisation of the surface of the spheres. On the other hand, those that have had a more intimate contact are crumbled (Fig. 4g). Since ButOH is adsorbed on pore and it is essential to produce HO• radicals that preform the attack to the polymer, we believe that an intimate contact between the polymer and these radicals takes place nearby these pores. These pores are actually the space between anatase nanoparticles, so this interaction could disassemble the hierarchical structure formed by the nanoparticles. Due to their small size and loss of coordination with TFAA, these nanoparticles are extremely reactive. This reactivity would increase further when losing the hierarchical structure as the nanoparticles become more unstable. As a consequence, we propose that they will try to coordinate with the ambient oxygen randomly, with no order. As a result, their surface becomes amorphous. Both ways of amorphisation of the TiO_2 surface could explain the loose of crystallinity observed by XRD (Fig. 3f). Also, as a result of the global amorphisation of the powder, it is no longer possible to detect the presence of brookite. Whether this implies a change in the brookite/anatase ratio is something that can not be determined from the XRD data, and it would actually be interesting to evaluate this possibility in a more realistic scenario working with microplastics in aqueous suspension (see "conclusions" section).

Focusing on the polymer, it is not spared from morphological changes either, since it is evident that it has been attacked or exfoliated when it came into contact with titanium. Its surface goes from smooth (Fig. 4b) to porous and pitted (Fig. 4g). These changes are reported to be related to a degradation of the polymer [2]. Indeed, they would allow TiO_2 to access to deeper layers of the polymer for further attack.

Another clue about a possible interaction between both materials lies in the other bands observed by emission photoluminescence (Fig. 2e). In fact, this technique is extremely sensitive to any chemical reaction or molecular adsorption taking place on the surface of semiconductors [43]. In accordance with the band assignment carried out by Serpone et al. and Kernazhitsky et al. [27,28], almost all relative intensities from band to band and recombination transitions decrease. Only the recombination band at 431 nm maintains a similar intensity but its width increases, which would imply that this process is favoured in a wider range of energies. A decrease in the available surface area (*i.e.* sphere breakage and/or adsorption of other species), an increase in the efficiency of charge separation near the surface by the adsorption of charged adsorbate, and the capture of holes generated in the measurement by chemisorbed surface hydroxyl groups, could be some of the reasons for the decrease in intensities [27]. In

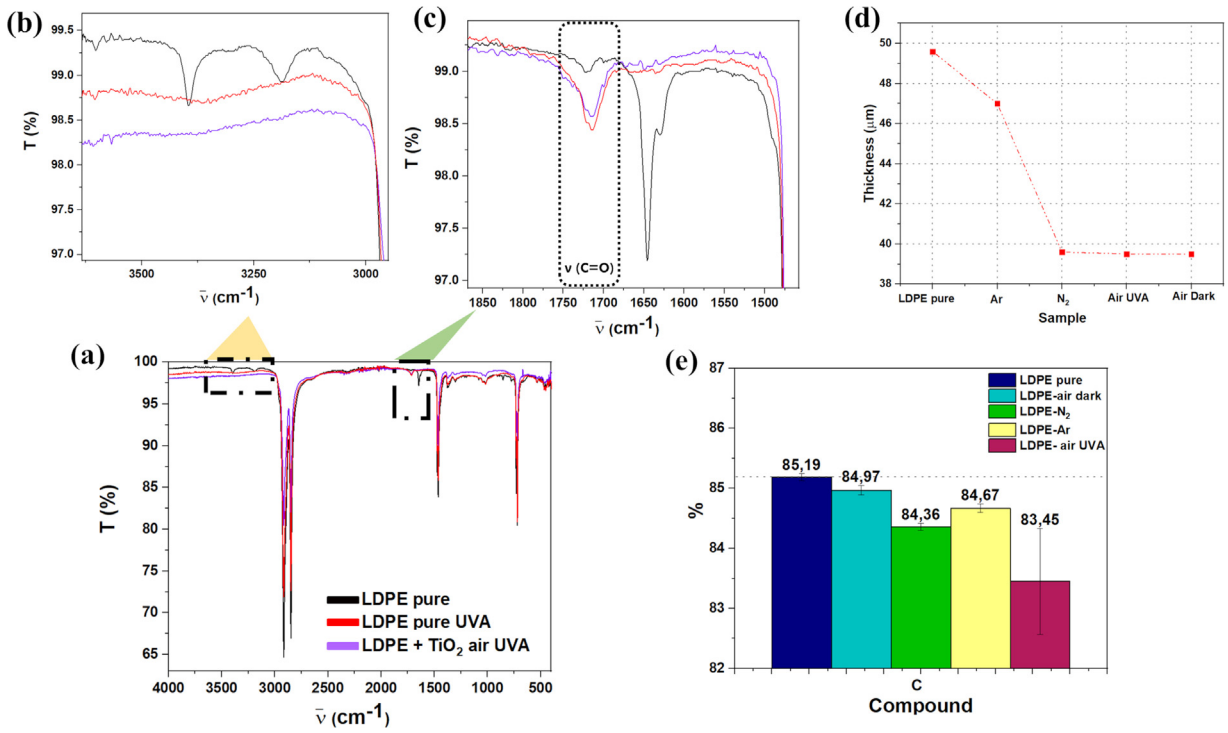

Fig. 5 – (a) FTIR-ATR spectra of LDPE pure under darkness (black) and under UVA radiation (red), LDPE after contacting TiO_2 in air atmosphere under UVA radiation (purple). FTIR-ATR zoom spectra in (b) the 3500–2500 cm^{-1} ν(O—H) and HALS area and (c) 1730–1600 cm^{-1} CO and HALS area. (d) Thickness of LDPE bag before and after contacting with TiO_2 under different environments. (e) Elemental chemical analysis of LDPE–TiO_2 system under different environments.

other words, when the TiO_2 is in contact with LDPE, an interaction occurs that creates an alternative pathway for electrons and holes generated during the measurement. This evidences an intimate interaction between the two materials. Finally, a fairly straightforward way to observe whether the interaction leads to degradation is to measure the thickness of the plastic bag together with the content of carbon. It is particularly interesting that the data reveal up to a 20% thickness reduction, from 49.6 μm to 39.5 μm (Fig. 5d) but a slight decrease of the percent of carbon, from 85.19% to 84.97% (Fig. 5e). This means that the spheres in this environment remove plastic from the bag, interact with it but do not degrade it in a comparable way. Nevertheless, some extent of the plastic is degraded.

Study of the LDPE–TiO_2 interaction: N_2/Ar atmosphere + darkness

According to the results obtained, the system is studied under inert atmospheres for a more comprehensive study of the role of oxygen. The first thing to consider in the interpretation and discussion of these results is the experimental setup and the permeability of the gases. Due to the experimental setup, LDPE + TiO_2 system under an Ar atmosphere is more isolated from atmospheric oxygen than the system under N_2 atmosphere. In addition, this plastic is more permeable to Ar, then to O_2 and finally to N_2 [44]. Thus, it is possible that the atmospheric oxygen diffuses into the N_2 system. In view of the above results, the presence of O_2 could have implications for plastic interaction and degradation. With this in mind, the yellow colouration of the ceramic powder is also observed in these environments. Although permeability to oxygen in the environment with N_2 to form the peroxy titanate complex is possible, this phenomenon would not be predominant enough to observe a yellow colouration. Moreover, in Ar's more impermeable environment, the presence of the complex could not be explained. Since in this experimental procedure vacuum is applied before changing the atmosphere, it is a parameter to consider. In fact, a pale-yellow colour is given to the virgin powder after vacuuming. This is correlated with the decrease in the intensity of υ(O—H) bands observed in the FTIR-ATR spectra (Fig. 2b black *vs* red curves), due to the desorption of water and ButOH from pore. The vacuum applied is not enough to evaporate these species, keeping a fraction of them adsorbed on the surface and thus giving colouration to the powder. When applying an Ar or N_2 atmosphere, the gas molecules displace in a greater way the ButOH on pore, increasing a little bit the υ(O—H) band (Fig. 2b light blue and orange curves respectively) with respect to the virgin powder after vacuum (Fig. 2b red curve). This displacement is greater with Ar due to its smaller size. Interestingly, when the ceramic is with LDPE in these inert atmospheres, the 3094 cm^{-1} band drops, leaving only the 3296 cm^{-1} band contribution. Both bands are related to υ(O—H) but higher wavelength implies higher bond strength. Therefore, we suggest that 3094 cm^{-1} is related to the υ(O—H) intermolecular of a hydrogen bond type interaction between the oxygen of a TiO_2 nanoparticle with the hydrogen of adsorbed water (Fig. 2f green) and/or a υ(O—H) intramolecular with a hydrogen of a Ti—OH bond inside

the same nanoparticle (Fig. 2f yellow). The 3296 cm^{-1} band would correspond instead to a υ(O—H) intermolecular between an O and H of two different nanoparticles inside the sphere (Fig. 2f pink). The fact that, in the presence of the polymer, the 3094 cm^{-1} band drops while the 3296 cm^{-1} band remains in inert atmosphere, means that there is an intramolecular contact (inside the nanoparticle) between the plastic and the TiO_2 (Fig. 2i) in contrast with the interaction in air atmosphere, between nanoparticles (Fig. 2g).

For the FTIR-ATR spectra of the polymer, a depletion of the HALS (3500–2900 cm^{-1} and 1644 cm^{-1}) and vinyl bands (855 cm^{-1}) is also observed (Fig. 3b and c). It also decreases the intensity of the typical polymer bands (Fig. 3a). In addition, the carbonyl band at 1715 cm^{-1} disappears in the N_2 environment but remains in the Ar one (Fig. 3c). This could be due to the permeability of oxygen in the former one. It is worth mentioning that no radical generation in an inert atmosphere and darkness has been reported [20,45] but since neither of these bands are observed in the powder spectra (Fig. 2a–c), these results evidence a clear degradation of the stabilisers. Neither is there much literature about the degradation mechanisms of LDPE in an inert atmosphere and the absence of light. However, some of the minority degradation pathways that occur in the presence of oxygen are reported to be prominent in the absence of oxygen. Some of them are the abstraction of hydrogen from another LDPE chain, transferring the radical by "radical hopping", and/or cross-linking instead of chain scission [4,41].

The effect of an inert atmosphere should not be neglected since a new diffraction maximum at 59.28° is observed in XRD pattern of the polymer (Fig. 3e). Analogously, the crystallinity of TiO_2 decreases in a similar way than in the air atmosphere (Fig. 3f). In contrast, the spheres are not as broken as they were in the air atmosphere and their surface looks cleaner (Fig. 4d and f), but the polymer film still looks attacked (Fig. 4h and j). We suggest that both the loss of crystallinity and stability of the spherical geometry are due to the interaction with the polymer. As mentioned, the vacuum allows the polymer to interact with ButOH without entering between the nanoparticles. As a result, the hierarchical structure might not suffer as much as in the air environment.

According to the emission photoluminescence spectra, a similar response of the material in these environments is observed. The relative intensity of the transitions behaves analogously to that observed in the oxygen atmosphere with respect to the original powder (Fig. S3). When comparing the nitrogen and argon environment with the air one (Fig. S4), the latter has a minor emission of photoluminescence (including oxygen vacancies). When comparing the two former ones, lower emission photoluminescence is observed in a nitrogen environment (Fig. S3). This implies, again, an intimate interaction between the two materials regardless of the atmosphere.

Focusing on the oxygen vacancies and following the reasoning of the previous section, their reduction should be accompanied by a stabilisation of the anatase octahedra and an increase to the typical ~3.2 eV band gap [14]. This phenomenon is indeed observed, having the highest band gap in the samples with the lowest number of oxygen vacancies: 3.25 eV (air) > 3.14 eV (nitrogen) > 3.08 eV (argon) > 3.04 eV (original powder). However, the weight gain associated with the filling of vacancies is not observed (Fig. 1j) because the weight loss associated with plastic degradation predominates (Fig. 5d and e). Up to a 20% thickness reduction, from 49.6 μm to 39.6 μm is observed in N_2 atmosphere, along with a decrease of the percent of carbon from 85.19% to 84.36%. In argon atmosphere, a slightly smaller reduction in the carbon percentage (84.67%) is appreciated along with a more considerably minor reduction of the thickness (47.0 μm). Interestingly, the behaviour of the materials in nitrogen environment reminds of the one observed in air, removing plastic from the bag beyond its degradation capacity. Instead, lower activity under argon environment takes place. This is consistent with the permeability of oxygen in the nitrogen system.

Study of the LDPE–TiO_2 interaction: photocatalysis

So far, plastic interaction and degradation have been observed in the dark and in aerobic and anaerobic environments. However, the influence of light on this process is particularly interesting considering that TiO_2 is widely known for its excellent photocatalytic properties. Due to its semiconductor nature, when it is irradiated with at least the same energy as its band gap, an electron from the valence band (VB) is promoted to the conduction band (CB), generating a hole (h^+) in the VB. The electron can diffuse to the surface and react with oxygen to generate oxygen anion radicals ($O_2\bullet^-$). Those radicals continue to react until they form $HO_2\bullet$ and H_2O_2 species. Regarding the holes, they generate OH• radicals by reacting with adsorbed water or by being trapped at the bridging oxygen anions. All these ROS species can break chemical bonds and degrade pollutants. However, it is believed that OH• radicals are the main responsible for the degradation of organic compounds [6,13].

In this scenario, it is logical to think that the first organic compounds to be degraded would be those already initially adsorbed on the surface, like ButOH or the peroxy titanate complex previously described in a similar way that the deactivation of the superoxide radicals [33]. The degradation of ButOH is evidenced by the decrease of the υ(OH) band in the FTIR-ATR spectra (Fig. 2b purple curve). Not only this degradation is logically favoured under radiation against darkness but it also seems that this environment attacks the CO groups of the TFAA adsorbed on the spheres (Fig. 2c). Following the explanation of "Study of the LDPE–TiO_2 interaction: air atmosphere + darkness" section, if this functional group is being degraded, the {0 0 1} facets of anatase are destabilised, the concentration of oxygen vacancies decreases, and the initial reduced band gap increases [7,31,32]. In fact, a 3.22 eV band gap is achieved, which is very close to the band gap obtained in darkness and air atmosphere. Instead, the degradation of the peroxy titanate complex can be seen in the lack of yellowing of the semiconductor (Fig. 1i).

There is evidence of the degradation not only of the adsorbed groups on the semiconductor but also of the plastic itself. The FTIR-ATR spectrum of the polymer shows the removal of HALS and vinyl groups, along with an increase in the intensity of the CO band (Fig. 5a–c purple curve). However, it should not be lost sight of the contribution of the LDPE photolysis. In fact, the empty bag in the same conditions suffers the same changes (Fig. 5a–c red curve). For the HALS photodegradation, Kamran et al. [6] propose a predominant

mechanism where a nitroxide radical reacts with OH• radicals to obtain a carbonyl group by further radical reactions. An OH• radical is also being reported to start the photodegradation mechanism of LDPE [14,15,34]. As a consequence, the hydrocarbon chain forms a radical and, through several radical reactions, it evolves into carbonyl groups (aldehyde, ketone or carboxyl acid). As mentioned, the photogeneration of OH• radicals is clear for a semiconductor, but for the empty bag, the hydrocarbon chain cannot absorb UV radiation on its own. Small unsaturations and carbonyl groups generated during the processing of the polymer at high temperatures act as chromophores. They absorb light and provoke the generation of radicals that start the photolysis of the plastic [4]. However, the CO band does not increase as much when the titanium is present. This could indicate partial removal of the CO formed or less advanced degradation.

Something similar happens with the crystallinity of the polymer. A comparable crystallinity degree is observed for both LDPE with and without TiO_2 under light. However, it is slightly superior with titanium, since the diffraction maximum at 59.28° appears (Fig. 3e). It is also worth noting that the semiconductor with no light can crystallise the polymer to the same extent. As far as the crystallinity of the ceramic is concerned, the same degree of amorphisation is observed so far (Fig. 3f). This effect has been previously related to the interaction LDPE–TiO_2. In fact, in this case a similar decrease in the emission photoluminescence intensity is observed, but it decreases more in darkness (Fig. S5). It makes sense considering that the presence of light allows organic species to degrade further, decreasing the adsorption of these compounds in the long-term and thus the alternative pathway for electrons is not as predominant. As a result, this interaction loses intensity by photoluminescence and the surface of the sphere looks cleaner (Fig. 4e).

Regarding the morphology of both materials, a degradation of the polymer is evidenced and the spherical geometry is better preserved (Fig. 4i) than in the dark (Fig. 4g). A faster degradation rate due to the e^-/h^+ generation, means that the plastic does not penetrate as deeply into the structure. As a result, the hierarchical structure does not suffer as much as in darkness.

Finally, this increased degradation achieved by UVA–visible light is clearly evidenced by both the thickness and carbon percentage results obtained (Fig. 5d and e). The empty LDPE bag under irradiation maintains the initial thickness (49.5 μm), whereas the same level of thickness reduction is obtained by contacting with titanium either under radiation or darkness (39.5 μm). However, an important difference between a dark and an irradiated scenario is noticed by chemical analysis. Radiation leads to the greatest carbon percentage reduction among all environments, up to 83.45% from 85.19% (Fig. 4e). It is also noted that in this scenario the measurement is accompanied by a higher experimental uncertainty. This is merely an indicator of a greater dispersion in the measurement. This is in full agreement with the heterogeneity of the photodegradation of plastic reported by Babaghayou et al. [37]. After all, it must not be ignored that the ceramic material is the main promoter of the plastic's photo-oxidation and it is not fully dispersed covering the entire area of the polymer film. Moreover, since it is a solid-state photo-oxidation process, the movement of radicals is much slower than in aqueous or gaseous media, being diffusion-controlled [40,46].

Conclusions

The results obtained in this work so far demonstrate that nanostructured microspheres of TiO_2 are a promising candidate for degradation of LDPE. Their hierarchical structure brings together the advantages of the reactivity of nanoparticles and the ease of material handling that micrometre size brings. Moreover, their high specific surface area and the species adsorbed on their surface have an important role in the interaction and degradation with LDPE.

In addition, this work sheds some light on the hitherto largely unnoticed ability of TiO_2 to work as a catalyst too and not only as a photocatalyst or as a catalyst support. In fact, this semiconductor has achieved a successful interaction and partial solid-state degradation in all scenarios, regardless of the atmosphere or the presence or absence of radiation. Nevertheless, each environment influences the TiO_2 response. The atmosphere influences mainly in the propagation route of the plastic degradation. An aerobic environment seems to promote the chain scission of the polymer whereas an anaerobic environment leads to a cross-linking. On the other hand, the presence or absence of light is a determining factor in the speed and mechanism of the polymer photo-oxidation process. When the powder is irradiated, the process is much faster and leads to carbonyl species, whereas under no radiation a depletion of carbonyl groups is achieved. Moreover, the role of HALS stabilisers in polymer degradation should also not be ignored, particularly in dark conditions; since their role is to protect the polymer by taking radicals, they undergo radical reactions that can be used for TiO_2 to precisely attack them and generate more radicals to escalate the plastic degradation process.

Finally, it should be mentioned that, independently of the specific environment, a significant modification (amorphisation) of the catalyst material is observed as a result of the interaction with the plastic, which affects its hierarchical structure and may even have changed the anatase/brookite ratio. This may compromise its reusability. However, to some extent, that may be associated with the use of a macro-sized plastic bag sample model and also because a TiO_2–LDPE solid-state interaction has been promoted. It would be interesting to further study this interaction in a more realistic scenario, for example by working with microplastic models in an aqueous suspension that would also favour the elimination of by-products.

Funding

The authors acknowledge the Project TED2021-132779B-I00 funded by MICIU/AEI/10.13039/501100011033 and by the European Union NextGenerationEU/PRTR. A. Castellanos-Aliaga also acknowledges the Grant FPU21/03335 funded by MICIU/AEI/10.13039/501100011033 and by the FSE+. We also thank the CSIC Hub CONEXIÓN-FOTOCATÁLISIS (OASIS) for support.

Conflict of interest

None declared.

Appendix A. Supplementary data

Supplementary data associated with this article can be found in the online version available at https://doi.org/10.1016/j.bsecv.2024.09.005.

REFERENCES

[1] N.M.L. Nohara, M.C. Ariza-Tarazona, E.R. Triboni, E.L. Nohara, J.F. Villarreal-Chiu, E.I. Cedillo-González, Are you drowned in microplastic pollution? A brief insight on the current knowledge for early career researchers developing novel remediation strategies, Sci. Total Environ. 918 (2024) 170382, http://dx.doi.org/10.1016/j.scitotenv.2024.170382.

[2] S.N. Dimassi, J.N. Hahladakis, M. Chamkha, M.I. Ahmad, M.A. Al-Ghouti, S. Sayadi, Investigation on the effect of several parameters involved in the biodegradation of polyethylene (PE) and low-density polyethylene (LDPE) under various seawater environments, Sci. Total Environ. 912 (2024) 168870, http://dx.doi.org/10.1016/j.scitotenv.2023.168870.

[3] K.N. Palansooriya, M.K. Sang, A. El-Naggar, L. Shi, S.X. Chang, J. Sung, W. Zhang, Y.S. Ok, Low-density polyethylene microplastics alter chemical properties and microbial communities in agricultural soil, Sci. Rep. 13 (2023) 16276, http://dx.doi.org/10.1038/s41598-023-42285-w.

[4] A.L. Andrady, K. Lavender Law, J. Donohue, B. Koongolla, Accelerated degradation of low-density polyethylene in air and in sea water, Sci. Total Environ. 811 (2022) 151368, http://dx.doi.org/10.1016/j.scitotenv.2021.151368.

[5] J.L. Hodgson, M.L. Coote, Clarifying the mechanism of the Denisov cycle: how do hindered amine light stabilizers protect polymer coatings from photo-oxidative degradation? Macromolecules 43 (2010) 4573–4583, http://dx.doi.org/10.1021/ma100453d.

[6] M. Kamran, M.A. Morsy, T.A. Kandiel, W. Iali, Semi-automated EPR system for direct monitoring the photocatalytic activity of TiO_2 suspension using TEMPOL model compound, Photochem. Photobiol. Sci. 21 (2022) 2071–2083, http://dx.doi.org/10.1007/s43630-022-00279-z.

[7] D.G. Calatayud, T. Jardiel, M. Peiteado, C.F. Rodríguez, M.R. Espino Estévez, J.M. Doña Rodríguez, F.J. Palomares, F. Rubio, D. Fernández-Hevia, A.C. Caballero, Highly photoactive anatase nanoparticles obtained using trifluoroacetic acid as an electron scavenger and morphological control agent, J. Mater. Chem. A: Mater. 1 (2013) 14358–14367, http://dx.doi.org/10.1039/c3ta12970e.

[8] D. Wiedmer, E. Sagstuen, K. Welch, H.J. Haugen, H. Tiainen, Oxidative power of aqueous non-irradiated TiO_2–H_2O_2 suspensions: methylene blue degradation and the role of reactive oxygen species, Appl. Catal. B 198 (2016) 9–15, http://dx.doi.org/10.1016/j.apcatb.2016.05.036.

[9] D.G. Calatayud, T. Jardiel, M. Rodríguez, M. Peiteado, D. Fernández-Hevia, A.C. Caballero, Soft solution fluorine-free synthesis of anatase nanoparticles with tailored morphology, Ceram. Int. 39 (2013) 1195–1202, http://dx.doi.org/10.1016/j.ceramint.2012.07.044.

[10] J. Alvarado, G. Acosta, F. Perez, Study of the effect of the dispersion of functionalized nanoparticles TiO_2 with photocatalytic activity in LDPE, Polym. Degrad. Stab. 134 (2016) 376–382, http://dx.doi.org/10.1016/j.polymdegradstab.2016.11.009.

[11] T. Jardiel, M. Peiteado, A. Castellanos-Aliaga, A.C. Caballero, D.G. Calatayud, Peptide-driven bio-assisted removal of metal oxide nanoparticles from an aqueous suspension: a novel strategy for water remediation, J. Clean. Prod. 285 (2021) 124852, http://dx.doi.org/10.1016/j.jclepro.2020.124852.

[12] Y. Tang, R. Cai, D. Cao, X. Kong, Y. Lu, Photocatalytic production of hydroxyl radicals by commercial TiO_2 nanoparticles and phototoxic hazard identification, Toxicology 406–407 (2018) 1–8, http://dx.doi.org/10.1016/j.tox.2018.05.010.

[13] P. Amato, M. Fantauzzi, F. Sannino, I. Ritacco, G. Santoriello, M. Farnesi Camellone, C. Imparato, A. Bifulco, G. Vitiello, L. Caporaso, A. Rossi, A. Aronne, Indirect daylight oxidative degradation of polyethylene microplastics by a bio-waste modified TiO_2-based material, J. Hazard. Mater. 463 (2024) 132907, http://dx.doi.org/10.1016/j.jhazmat.2023.132907.

[14] B.E. Llorente-García, J.M. Hernández-López, A.A. Zaldívar-Cadena, C. Siligardi, E.I. Cedillo-González, First insights into photocatalytic degradation of HDPE and LDPE microplastics by a mesoporous N–TiO_2 coating: effect of size and shape of microplastics, Coatings 10 (2020) 658, http://dx.doi.org/10.3390/coatings10070658.

[15] D. Wang, P. Zhang, M. Yan, L. Jin, X. Du, F. Zhang, Q. Wang, B. Ni, C. Chen, Degradation mechanism and properties of debris of photocatalytically degradable plastics LDPE–TiO_2 vary with environments, Polym. Degrad. Stab. 195 (2022) 109806, http://dx.doi.org/10.1016/j.polymdegradstab.2021.109806.

[16] D.G. Calatayud, T. Jardiel, M. Peiteado, A.C. Caballero, D. Fernández-Hevia, Microwave-induced fast crystallization of amorphous hierarchical anatase microspheres, Nanoscale Res. Lett. 9 (2014) 1–5, http://dx.doi.org/10.1186/1556-276X-9-273.

[17] A. Caballero Cuesta, A. Castellanos Aliaga, D. González Calatayud, M.T. Jardiel Rivas, M. Peiteado López, M.P. Villegas Gracia, TIO_2 Microspheres, Method of Obtaining Said TIO_2 Microspheres, and use Thereof as a Solar Photocatalyst, PCT/ES2023/070519, 2024.

[18] A. Caballero Cuesta, A. Castellanos Aliaga, D. González Calatayud, M.T. Jardiel Rivas, M. Peiteado López, M.P. Villegas Gracia, Microesferas de TiO_2, método de obtención de dichas microesferas de TiO_2 y uso como fotocatalizador solar, P202230763, 2022.

[19] Pike Technologies, Application Note – 0502. Calculating the Thickness of Free-Standing Films by FTIR, PIKE Technologies Spectroscopic Creativity (1998).

[20] I. Fenoglio, G. Greco, S. Livraghi, B. Fubini, Non-UV-induced radical reactions at the surface of TiO_2 nanoparticles that may trigger toxic responses, Chemistry 15 (2009) 4614–4621, http://dx.doi.org/10.1002/chem.200802542.

[21] S.S. Ali, I.A. Qazi, M. Arshad, Z. Khan, T.C. Voice, C.T. Mehmood, Photocatalytic degradation of low density polyethylene (LDPE) films using titania nanotubes, Environ. Nanotechnol. Monit. Manag. 5 (2016) 44–53, http://dx.doi.org/10.1016/j.enmm.2016.01.001.

[22] S.M. El-Sheikh, T.M. Khedr, G. Zhang, V. Vogiazi, A.A. Ismail, K. O'Shea, D.D. Dionysiou, Tailored synthesis of anatase–brookite heterojunction photocatalysts for degradation of cylindrospermopsin under UV–Vis light, Chem. Eng. J. 310 (2017) 428–436, http://dx.doi.org/10.1016/j.cej.2016.05.007.

[23] C. Ioakeimidis, K.N. Fotopoulou, H.K. Karapanagioti, M. Geraga, C. Zeri, E. Papathanassiou, F. Galgani, G. Papatheodorou, The degradation potential of PET bottles in the marine environment: an ATR-FTIR based approach, Sci. Rep. 6 (2016) 23501, http://dx.doi.org/10.1038/srep23501.

[24] D.G. Calatayud, R. Flores Martin, A. Castellanos-Aliaga, M. Peiteado, F.J. Palomares, A.C. Caballero, T. Jardiel, Tailoring the visible light photoactivity of un-doped defective TiO_2 anatase nanoparticles through a simple two-step solvothermal process, Nanotechnology 31 (2019) 045603, http://dx.doi.org/10.1088/1361-6528/ab49af.
[25] S. Yang, W. Tang, Y. Ishikawa, Q. Feng, Synthesis of titanium dioxide with oxygen vacancy and its visible-light sensitive photocatalytic activity, Mater. Res. Bull. 46 (2011) 531–537, http://dx.doi.org/10.1016/j.materresbull.2011.01.004.
[26] L. Aïnouche, L. Hamadou, A. Kadri, N. Benbrahim, D. Bradai, Ti^{3+} states induced band gap reduction and enhanced visible light absorption of TiO_2 nanotube arrays: effect of the surface solid fraction factor, Sol. Energy Mater. Sol. Cells 151 (2016) 179–190, http://dx.doi.org/10.1016/j.solmat.2016.03.013.
[27] L. Kernazhitsky, V. Shymanovska, T. Gavrilko, V. Naumov, L. Fedorenko, V. Kshnyakin, J. Baran, Room temperature photoluminescence of anatase and rutile TiO_2 powders, J. Lumin. 146 (2014) 199–204, http://dx.doi.org/10.1016/j.jlumin.2013.09.068.
[28] N. Serpone, D. Lawless, R. Khairutdinov, Size effects on the photophysical properties of colloidal anatase TiO_2 particles: size quantization or direct transitions in this indirect semiconductor? J. Phys. Chem. 99 (1995) 16646–16654, http://dx.doi.org/10.1021/j100045a026.
[29] C. Randorn, S. Wongnawa, P. Boonsin, Bleaching of methylene blue by hydrated titanium dioxide, ScienceAsia 30 (2004) 149–156, http://dx.doi.org/10.2306/scienceasia1513-1874.2004.30.149.
[30] E.M. Samsudin, S.B.A. Hamid, J.C. Juan, W.J. Basirun, A.E. Kandjani, S.K. Bhargava, Effective role of trifluoroacetic acid (TFA) to enhance the photocatalytic activity of F-doped TiO_2 prepared by modified sol–gel method, Appl. Surf. Sci. 365 (2016) 57–68, http://dx.doi.org/10.1016/j.apsusc.2016.01.016.
[31] A. El Mesoudy, D. Machon, A. Ruediger, A. Jaouad, F. Alibart, S. Ecoffey, D. Drouin, Band gap narrowing induced by oxygen vacancies in reactively sputtered TiO_2 thin films, Thin Solid Films 769 (2023) 139737, http://dx.doi.org/10.1016/j.tsf.2023.139737.
[32] Á. Morales-García, A. Macià Escatllar, F. Illas, S.T. Bromley, Understanding the interplay between size, morphology and energy gap in photoactive TiO_2 nanoparticles, Nanoscale 11 (2019) 9032–9041, http://dx.doi.org/10.1039/c9nr00812h.
[33] D. Pirozzi, C. Imparato, G. D'Errico, G. Vitiello, A. Aronne, F. Sannino, Three-year lifetime and regeneration of superoxide radicals on the surface of hybrid TiO_2 materials exposed to air, J. Hazard. Mater. 387 (2020) 121716, http://dx.doi.org/10.1016/j.jhazmat.2019.121716.
[34] P. Kaewkam, A. Kanchanapaetnukul, J. Khamyan, N. Phadmanee, K.Y.A. Lin, K. Kobwittaya, S. Sirivithayapakorn, UV-assisted TiO_2 photocatalytic degradation of virgin LDPE films: effect of UV-A, UV-C, and TiO_2, J. Environ. Chem. Eng. 10 (2022) 108131, http://dx.doi.org/10.1016/j.jece.2022.108131.
[35] J.V. Gulmine, P.R. Janissek, H.M. Heise, L. Akcelrud, Polyethylene characterization by FTIR, Polym. Test. 21 (2002) 557–563, http://dx.doi.org/10.1016/S0142-9418(01)00124-6.
[36] M.N. Miranda, M.J. Sampaio, P.B. Tavares, A.M.T. Silva, M.F.R. Pereira, Aging assessment of microplastics (LDPE, PET and uPVC) under urban environment stressors, Sci. Total Environ. 796 (2021) 148914, http://dx.doi.org/10.1016/j.scitotenv.2021.148914.
[37] M.I. Babaghayou, A.H.I. Mourad, V. Lorenzo, M.U. de la Orden, J. Martínez Urreaga, S.F. Chabira, M. Sebaa, Photodegradation characterization and heterogeneity evaluation of the exposed and unexposed faces of stabilized and unstabilized LDPE films, Mater. Des. 111 (2016) 279–290, http://dx.doi.org/10.1016/j.matdes.2016.08.065.
[38] S. Garnai Hirsch, B. Barel, E. Segal, Characterization of surface phenomena: probing early stage degradation of low-density polyethylene films, Polym. Eng. Sci. 59 (2019) E1–E475, http://dx.doi.org/10.1002/pen.24886.
[39] A.D. Vital-Grappin, M.C. Ariza-Tarazona, V.M. Luna-Hernández, J.F. Villarreal-Chiu, J.M. Hernández-López, C. Siligardi, E.I. Cedillo-González, The role of the reactive species involved in the photocatalytic degradation of HDPE microplastics using C, N-TiO_2 powders, Polymers (Basel) 13 (2021) 999, http://dx.doi.org/10.3390/polym13070999.
[40] P. Bracco, L. Costa, M.P. Luda, N. Billingham, A review of experimental studies of the role of free-radicals in polyethylene oxidation, Polym. Degrad. Stab. 155 (2018) 67–83, http://dx.doi.org/10.1016/j.polymdegradstab.20S18.07.011.
[41] G. Grause, M.-F. Chien, C. Inoue, Changes during the weathering of polyolefins, Polym. Degrad. Stab. 181 (2020) 109364, http://dx.doi.org/10.1016/j.polymdegradstab.2020.109364.
[42] M. Hamouya, A. Mahir, M. Chafik, E.L. Idrissi, Natural ageing of stabilized and unstabilized LDPE films: XRD and SEM analysis, Int. J. Res. Eng. Technol. 3 (2014) 210–215, http://www.ijret.org [accessed 15.06.24].
[43] D.K. Pallotti, L. Passoni, P. Maddalena, F. Di Fonzo, S. Lettieri, Photoluminescence mechanisms in anatase and rutile TiO_2, J. Phys. Chem. C 121 (2017) 9011–9021, http://dx.doi.org/10.1021/acs.jpcc.7b00321.
[44] J.H. Lee, Y.W. Kim, J.K. Jung, Investigation of the gas permeation properties using the volumetric analysis technique for polyethylene materials enriched with pure gases under high pressure: H_2, He, N_2, O_2 and Ar, Polymers (Basel) 15 (2023) 4019, http://dx.doi.org/10.3390/polym15194019.
[45] P.-W. Huang, N. Tian, T. Rajh, Y.-H. Liu, G. Innocenti, C. Sievers, A.J. Medford, M.C. Hatzell, Formation of carbon-induced nitrogen-centered radicals on titanium dioxide under illumination, JACS Au 3 (2023) 3283–3289, http://dx.doi.org/10.1021/jacsau.3c00556.
[46] M. Raab, V. Hnfit, E. Schmidt, L. Kotulfik, L. Taimr, J. Pospi~il, The action of anthraquinone sensitizers in the photo-oxidative degradation of low density polyethylene: mechanical evidence of dark processes, Polym. Degrad. Stab. 18 (1987) 123–134, http://dx.doi.org/10.1016/0141-3910(87)90025-5.